

# Electronic Nematicity Revealed by Torque Magnetometry in Iron Arsenide $\text{EuFe}_2(\text{As}_{1-x}\text{P}_x)_2$

Xiaofeng Xu<sup>1</sup>, W. H. Jiao<sup>2</sup>, N. Zhou<sup>1</sup>, Y. K. Li<sup>1</sup>, B. Chen<sup>3,1</sup>, C. Cao<sup>1</sup>, Jianhui Dai<sup>1</sup>, A. F. Bangura<sup>4</sup>, Guanghan Cao<sup>2</sup>

<sup>1</sup>*Department of Physics, Hangzhou Normal University,  
Hangzhou 310036, China*

<sup>2</sup>*State Key Lab of Silicon Materials and Department of Physics,  
Zhejiang University, Hangzhou 310027, China*

<sup>3</sup>*Department of Physics,  
University of Shanghai for Science & Technology, Shanghai, China*

<sup>4</sup>*RIKEN(The Institute of Physical and Chemical Research),  
Wako, Saitama 351-0198, Japan.*

(Dated: February 19, 2014)

Electronic nematics, an electron orientational order which breaks the underlying rotational symmetry, have been observed in iron pnictide superconductors several years after their discovery. However, the universality of the doping dependence of this phase and its relation to other symmetry-breaking orders (such as superconductivity) in distinct families of iron pnictides, remain outstanding questions. Here we use torque magnetometry as a probe to study the rotational symmetry breaking in  $\text{EuFe}_2(\text{As}_{1-x}\text{P}_x)_2$  without introducing external pressure. The nematic phase is found to proliferate well above the structural transition and to persist into the superconducting regime at optimal doping, after which it becomes absent or very weak, in sharp contrast to the behaviour observed in  $\text{BaFe}_2(\text{As}_{1-x}\text{P}_x)_2$ . These measurements suggest a putative quantum nematic transition near optimal doping under the superconducting dome.

The electronic nematic phase, an emergent quantum state in which rotational invariance is broken spontaneously and the electron fluid exhibits orientational order, has recently attracted a great deal of attention, largely due to its close proximity to the superconducting phase in both high- $T_c$  cuprates and iron pnictides[1–11]. In cuprates, electronic anisotropy sets in upon opening of the pseudogap, as nicely observed by the Nernst effect measurements on detwinned  $\text{YBa}_2\text{Cu}_3\text{O}_y$ [2]. In iron pnictides, despite the growing evidence for nematicity borne out by resistivity measurements under stress or strain[5, 7, 8], neutron scattering[10], shear modulus[11, 12], and Raman spectroscopy[13], relatively little is known about its universality amongst different families or even its microscopic origin.

Torque magnetometry proves to be a powerful thermodynamic tool for studying any anisotropic susceptibility in materials[6, 14, 15]. From a thermodynamic point of view, magnetic torque is the first derivative of free energy with respect to angular displacement and as such, tends to be zero in an isotropic material. This is because the torque as given by  $\tau = M \times H$ , has  $M$  (the magnetization) aligned parallel to  $H$  (the applied field)[16]. The torque therefore only develops whenever any anisotropy sets in. In real cases, the anisotropy may come from two distinct sources, one from external impurities and the other from an anisotropic electronic state[6]. Considering a situation where the magnetic field is rotating in the  $ab$  plane of a crystal, see the schematic illustration in Fig. 1(a), (the lowest order  $2\phi$  component of) the torque can be written as[6]:

$$\begin{aligned}\tau_{2\phi} &= A \cos 2(\phi + \phi_0) \\ &= A_{nem} \cos 2(\phi + \phi_{nem}) + A_{ext} \cos 2(\phi + \phi_{ext})(1)\end{aligned}$$

Here the first and the second terms correspond to the electron nematics and external contributions, respectively.  $A$ ,  $A_{nem}$ ,  $A_{ext}$  denote the amplitudes with initial phase  $\phi_0$ ,  $\phi_{nem}$ ,  $\phi_{ext}$  accordingly. Essentially, the nematic contribution may arise from two channels, the difference in  $\chi_{aa}$  and  $\chi_{bb}$ , as well as the off-diagonal  $\chi_{ab}$ , viz.,  $A_{nem} \cos 2(\phi + \phi_{nem}) = \frac{1}{2} H^2 [(\chi_{aa} - \chi_{bb}) \sin 2\phi - 2\chi_{ab} \cos 2\phi]$ , although it turns out that only  $\chi_{ab}$  comes into play in iron pnictides[6]. It is worth noting that  $\phi_{nem}$  and  $\phi_{ext}$  are both temperature independent. As a result, the phase  $\phi_0$  will solely depend on the relative weight between  $A_{nem}$  and  $A_{ext}$ . In other words,  $\phi_0$  undergoes a significant shift from  $\phi_{ext}$  once the nematic  $A_{nem}$  develops a non-zero value. Physically, this is exactly what was used to identify the nematic phase in  $\text{BaFe}_2(\text{As}_{1-x}\text{P}_x)_2$ [6].

The material in question in this study is a prototypical 122-family iron pnictide  $\text{EuFe}_2(\text{As}_{1-x}\text{P}_x)_2$ [17–21]. In the *parent*  $\text{EuFe}_2\text{As}_2$  compound, the high-temperature tetragonal phase undergoes structural and magnetic transitions coincidentally below  $T_s$  ( $=T_N$ ). Upon isovalent P substitution on As sites, both  $T_s$  and  $T_N$  are gradually suppressed and superconductivity emerges, reaching a maximum superconducting transition temperature  $T_c$  of  $\sim 30$  K at optimal doping level of  $x \sim 0.2$ [19, 20]. This gives a phase diagram akin to the one generic to 122 family. In addition, the rare earth  $\text{Eu}^{2+}$  develops a

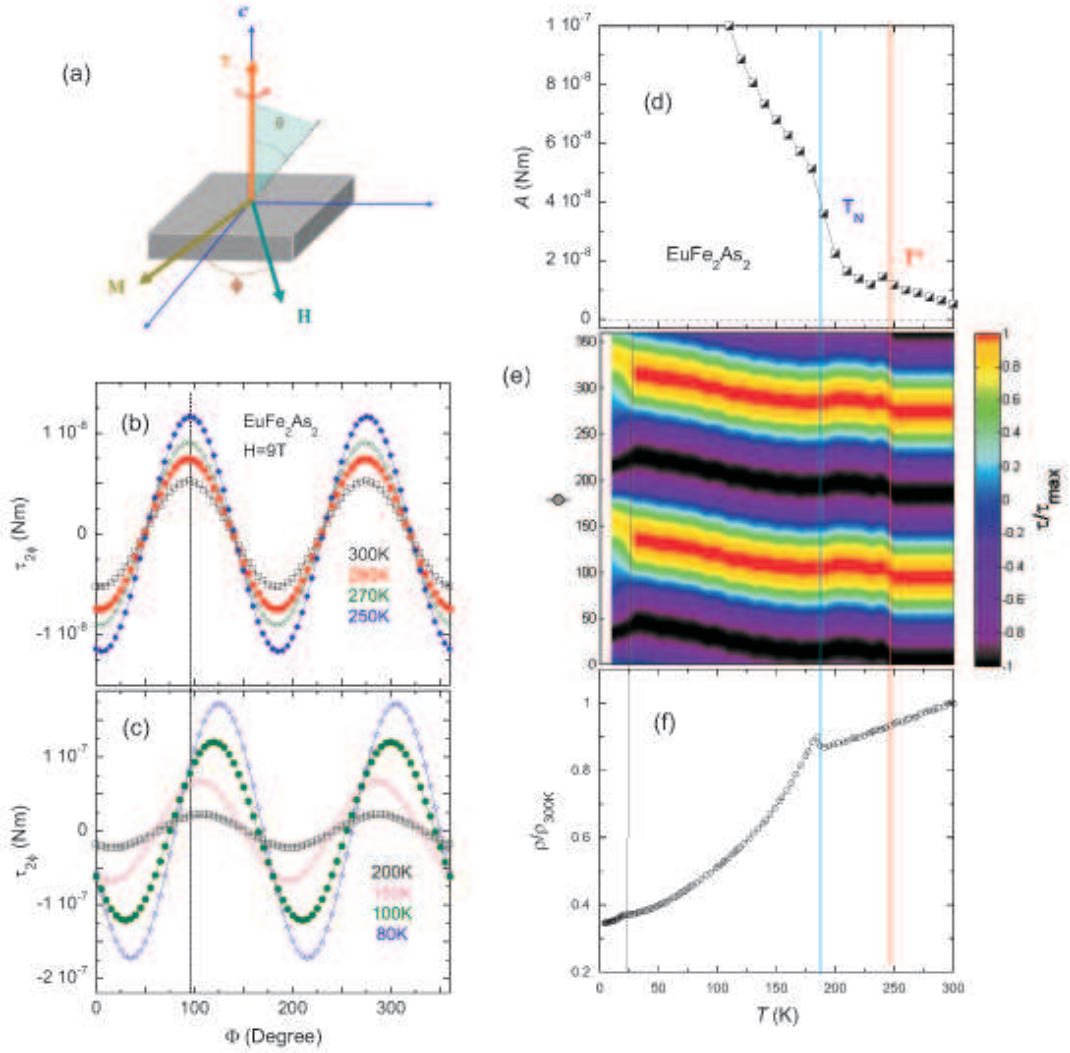


FIG. 1: (Color online) The angular dependence of magnetic torque with fields rotating in the  $ab$  plane of  $\text{EuFe}_2\text{As}_2$  parent compound. **(a)** The schematic diagram for the field orientation in the setup. Note the  $x$ - and  $y$ -axes do not necessarily denote the crystal  $a$ -axis and  $b$ -axis due to the lack of the knowledge about the crystalline axes in the plane which however will not affect our conclusions in the main text. **(b)** and **(c)** show the angular dependence of the torque above and below the nematic onset temperature  $T^*$ , respectively. **(d)**. The temperature dependence of the amplitude  $A$  (see Eqn. (1)). **(e)**. The contour plot of the torque as a function of both temperature and angle. Note the torques are renormalized to the maximal values at each temperature. **(f)**. The zero-field resistivity for the strain-free sample.

magnetic ordering at low temperature  $\sim 20\text{ K}$ . Intriguingly, this magnetic order evolves with P doping level, antiferromagnetically (AFM) coupled at low P concentrations and ferromagnetically (FM) on the overdoped side [19, 21].

Here we use the temperature evolution of the angular magnetic torque to detect the possible nematic phase above  $T_s$  in  $\text{EuFe}_2(\text{As}_{1-x}\text{P}_x)_2$  (see Supplementary Information (SI) for experimental details). The initial phase of the magnetic torque  $\phi_0$  was seen to be significantly shifted below  $T^*$ , a new temperature scale signifying the onset of the nematic order, which is well above  $T_s$  and  $T_N$ . This nematic order was found to decrease with increasing P concentrations up to the optimal doping and

to become very weak (or even absent) in the overdoped region. The resultant phase diagram suggests a possible quantum nematic transition beneath the superconducting dome, which in turn may have an intimate connection with the observed superconductivity.

The panels (b) and (c) in Figure 1 show the representative angular torque at various fixed temperatures under 9 tesla field for the parent compound  $\text{EuFe}_2\text{As}_2$ . Clearly, a magnetic torque is manifest even at 300 K, indicative of the considerable anisotropy of the magnetization at room temperature. With decreasing temperatures, the sinusoidal torque gets larger while kept at a constant phase. However, this angular profile alters significantly below  $\sim 250\text{ K}$ , as shown in Fig. 1(c). The phase is

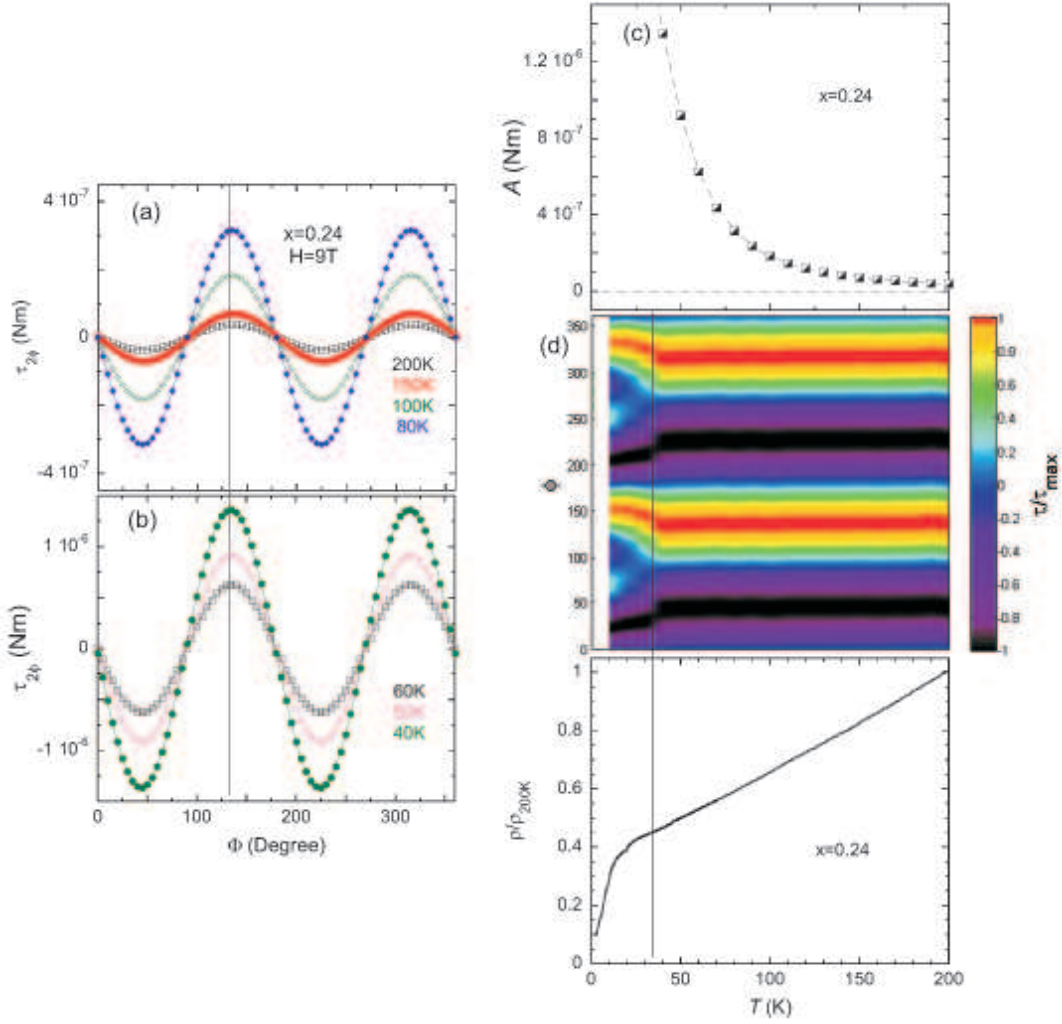


FIG. 2: (Color online) The angular dependence of the torque for fields rotating in the  $ab$  plane of the overdoped sample ( $x=0.24$ ). (a) and (b). The angular torque at different temperatures. (c) summarizes the resultant amplitude  $A$  at each temperature studied. (d). The contour plot of the renormalized torque as a function of temperature and angle. (e) presents the zero-field resistivity for strain-free sample.

no longer *locked* into the high- $T$  one and evidently seen to vary with temperatures. This fundamental change of the angular torque is best visualized in a contour plot presented in Fig. 1(e) where the data are renormalized to their maximal values at each individual temperature,  $\tau/\tau_{max}(T)$ . The temperature dependence of the amplitude  $A$  (see Eqn. (1)) and the zero-field resistivity  $\rho(T)$  for a stress-free sample were also incorporated as Fig. 1 (d) and (f), respectively. In spite of the smooth  $\rho(T)$  curve across  $\sim 250$  K, a new temperature scale, marked as  $T^*$ , manifests itself as a kink in  $A(T)$  in Fig. 1(d) and the considerable change of the angular torque profile in Fig. 1(e). The structural transition at  $T_s(\sim T_N) \sim 180$  K, displays in Fig. 1 (d) as a sharp increase in  $A(T)$ , in Fig. 1(e) as a inflexion point, and in Fig. 1 (f) as an upturn in the resistivity. As the temperature is lowered down to  $\sim 20$  K,  $\rho(T)$  undergoes a moderate kink, associated with

the magnetic order of  $\text{Eu}^{2+}$  ions. This magnetic order also has profound effects on the torque data (Fig. 1 (e)) by introducing a large 4-fold angular component (see SI).

The above phenomenon can overall be understood in the preceding dichotomy analysis. At high temperatures, only the torque from external impurities takes a role therefore it will maintain the same phase  $\phi_{ext}$ . As the sample is cooled below  $T^*$ , a second nematic contribution sets in such that the phase will shift to  $\phi_0$  which is distinct from the high- $T$   $\phi_{ext}$ . Apparently, this new phase  $\phi_0$  depends on the relative weights of the two contributions. In this sense,  $T^*$  corresponds to the onset temperature for the electronic nematic phase.

In order to confirm that only the  $ab$  plane is responsible for the above findings, we perform the field rotation out of the FeAs plane (data shown in SI). Interestingly, the phase of this angle-dependent torque barely changes with

temperature, in stark contrast to the case of in-plane field rotation. Collectively, these provide compelling evidence for the nematic origin of the phase shift observed upon in-plane rotation.

Similarly, we also studied the in-plane angular evolution of the magnetic torque in underdoped ( $x=0.18$ ,  $T_c=21$  K) and nearly optimally-doped ( $x=0.2$ ,  $T_c=29$  K) samples. Similar phase shifts were also observed in these two doping levels, although at much lower temperatures. The onset temperatures for the nematic phase,  $T^*$ , were identified as  $\sim 140$  K and  $\sim 100$  K, respectively (see SI). Although  $T^*$  for the optimally-doped sample remains high, the relative phase shift below  $T^*$  gets much smaller, indicative of the weak nematicity.

We next consider an overdoped sample ( $x=0.24$ , determined from EDX, see SI) whose resistivity, Fig. 2(e), starts an incipient dip at  $\sim 20$  K and a quick drop below  $\sim 14$  K but non-zero resistivity is observed down to 2.5 K, indicating either sample inhomogeneity or strong internal field induced by  $\text{Eu}^{2+}$  FM ordering on the overdoped side[17, 19]. Angular torque in the normal state (Fig. 2 (a) and (b)) is sinusoidal and maintains the same phase all the way down to the superconducting (fluctuation) temperature, below which a substantial 4-fold component develops (see SI for the torque in the superconducting state). It is noted that this 4-fold symmetry torque sets in about  $10\sim 20$  K above  $T_c$ , similar to what was observed in  $x=0.18$  and  $x=0.2$  samples. We attribute this to the superconducting fluctuations which have the same effects on the torque as the  $\text{Eu}^{2+}$  order in the parent compound. Overall, this locking of the torque phase with temperature is vividly captured in the contour plot, Fig. 2 (d). On the other hand, the temperature dependence of the amplitude,  $A(T)$  in Fig. 2 (c), evolves in a smooth manner in the normal state.

Figure 3 shows the revised phase diagram of  $\text{EuFe}_2(\text{As}_{1-x}\text{P}_x)_2$  revealed from our torque measurements. In addition to the phases uncovered thus far by other measurements, we have found a rather broad region above the structural and magnetic transitions where the electrons in the FeAs plane start to develop a novel, orientational order that breaks the rotational invariance of the underlying tetragonal lattice and reduce the symmetry from  $C_4$  to  $C_2$ [4]. This nematic phase is found to extend all the way up to the optimal doping where the structural and magnetic transitions are believed to be completely suppressed. On the overdoped side, however, no nematic phase can be revealed above the superconducting transition, in contrast to the phase diagram of  $\text{BaFe}_2(\text{As}_{1-x}\text{P}_x)_2$  where nematicity clearly survives in the very overdoped region[6]. This indicates that the phase diagram associated with the nematic order is not universal, even within the 122-family.

We note that the electronic anisotropy above the structural and magnetic transitions has also been investigated by a thermoelectric power (TEP) study in three spec-

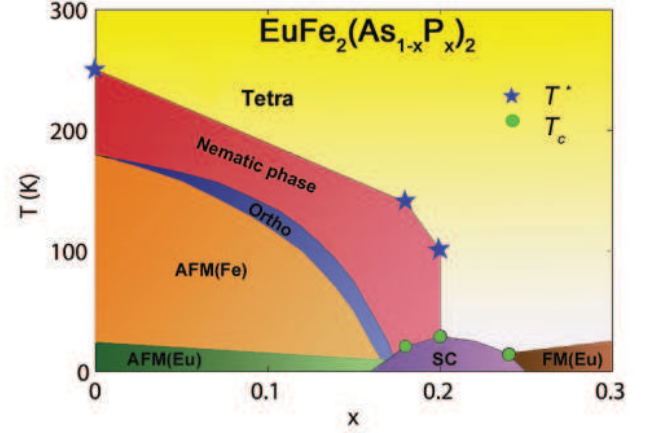


FIG. 3: (Color online) The resultant phase diagram of  $\text{EuFe}_2(\text{As}_{1-x}\text{P}_x)_2$  as derived collectively from our measurements and the previous studies. For simplicity, we neglect the fine spin structure of  $\text{Eu}^{2+}$ , including that in the superconducting state, which were recently uncovered in Ref. [21, 22].

imens of  $\text{EuFe}_2(\text{As}_{1-x}\text{P}_x)_2$ , two non-superconducting samples ( $x=0.05$  and  $0.09$ ) and one overdoped sample ( $x=0.23$ )[23]. Similarly, the nematic phase had only been detected in the  $x=0.05$  and  $x=0.9$  samples, no anisotropy being observed in the overdoped  $x=0.23$  sample. Remarkably, for  $x=0.05$ , the anisotropy in the TEP appears to develop even above  $\sim 250$  K, a temperature we assigned as  $T^*$  for the onset temperature of the nematicity in the parent compound (Note that the TEP was performed under a uniaxial stress clamp. It may effectively enhance the nematicity[23]). Consistently, on the overdoped side, no nematic order can be detected in the TEP measurements nor our magnetic torque study. For the TEP measurements, it is difficult to define the onset temperature  $T^*$  since the uniaxial pressure is necessary to detwin the sample. However, thanks to the unbalanced twin-domain volumes, torque measurements prove to be an effective approach to study any anisotropy in a stress-free sample[6].

It is unlikely that the absence of the nematicity on the overdoped side is due to the sample inhomogeneity. First, the non-zero resistivity below  $T_c$  in our sample does not necessarily imply the sample inhomogeneity as the internal field induced by  $\text{Eu}^{2+}$  FM order in overdoped sample may be comparable to the upper critical field. Second, no nematicity has either been detected by the TEP study in the overdoped sample, whose sample homogeneity is not a serious issue there[23]. Moreover, it is noteworthy that even under the uniaxial stress, no resistivity anisotropy has been observed in the overdoped 122 samples, including Co and Ni doped  $\text{BaFe}_2\text{As}_2$ [8].

A natural question raised by our study concerns the relation between these various transitions in the phase diagram and the microscopic origin of the nematicity.

As argued in Ref. [6], because  $C_4$  rotational symmetry can only be broken once, the structural distortion in the diagram is not a real phase transition, but rather a transition dubbed 'meta-nematic transition' in which the order parameter has a sharp increase *albeit* it is non-zero on either side of the transition. Instead, the nematic transition is the genuine second-order transition because the order parameter (proportional to  $A_{nem}$  in the torque) is only non-zero below  $T^*$ . This is further confirmed by the divergent nematic susceptibility, and the nematic order is considered as the driving force behind the structural instability[7].

The origin of this electronic anisotropy is highly controversial to date and two alternative proposals have been widely discussed. In the Ising-nematic scenario[24–28], the nematic phase is characterized by a broken  $Z_2$  Ising symmetry (spins differentiate in the otherwise equivalent directions and are apt to point along one of the in-plane axes) and is driven by spin fluctuations above the AFM order of Fe. In the other theory[29–31], it is the ferro-orbital ordering, uneven population of the  $d_{xz}$  and  $d_{yz}$  orbitals, that gives rise to the nematicity which ultimately makes the orthorhombic crystal lattice energetically more stable. For the present system, the nematic order clearly survives to the optimal doping where the long-range AFM order is thought to be completely suppressed. However, quantum spin fluctuations can still in principle induce the nematicity in this regime. How the quantum fluctuations play a role in the highly overdoped  $\text{BaFe}_2(\text{As}_{1-x}\text{P}_x)_2$ , warrants further theoretical insights. Alternatively, if the orbital ordering is the driving force[28], the termination of the nematic phase near optimal doping is somehow puzzling. Whether the disappearance of the nematic phase is related to a Lifshitz transition near this doping region remains to be seen[23, 32]. It is worth noting that recent TEP experiments seemingly disagree with the orbital-ordering proposal as the origin of nematicity because it does not match the sign of the TEP anisotropy above  $T_s$ [23]. The contrasting doping dependence of the nematic phase in 122-families also imposes stringent challenges on any theory which relies on orbital-ordering.

To conclude, magnetic torque measured in  $\text{EuFe}_2(\text{As}_{1-x}\text{P}_x)_2$  reveals a new phase boundary associated with nematic phase formation up to the optimal superconducting transition. This nematic transition is not present in the overdoped side of the phase diagram, heralding a possible quantum (nematic) transition near optimal doping concentration[33]. Indeed, quantum critical points have been uncovered in iron pnictides, in particular for the 122-families, near to the optimal doping[34–38]. Future studies are therefore needed to clarify whether the nematic fluctuations associated with this quantum nematic transition are the fundamental ingredient for its enhanced superconductivity[39, 40].

We thank N. E. Hussey, C. M. J. Andrew, C. Lester,

Xiaofeng Jin for stimulating discussions. This work is sponsored by the NSFC (Grant No. 11104051, 11104053).

- 
- [1] P. A. Lee, N. Nagaosa, X. G. Wen, *Rev. Mod. Phys.* **78**, 17 (2006).
  - [2] R. Daou *et al.*, *Nature*. **463**, 519 (2010).
  - [3] R. A. Cooper *et al.*, *Science* **323**, 603 (2009).
  - [4] E. Fradkin, S. A. Kivelson, M. J. Lawler, J. P. Eisenstein, and A. P. Mackenzie, *Annu. Rev. Condens. Matter Phys.* **1**, 153 (2010).
  - [5] J. H. Chu, J. G. Analytis, K. De Greve, P. L. McMahon, Z. Islam, Y. Yamamoto, and I. R. Fisher, *Science* **329**, 824 (2010).
  - [6] S. Kasahara *et al.*, *Nature* **486**, 382 (2012).
  - [7] J. H. Chu, H. H. Kuo, J. G. Analytis, and I. R. Fisher, *Science* **337**, 710 (2012).
  - [8] H. H. Kuo *et al.*, *Phys. Rev. B* **84**, 054540 (2011).
  - [9] M. Yi *et al.*, *Proc. Natl Acad. Sci. USA* **108**, 6878 (2011).
  - [10] H. Q. Luo *et al.*, *Phys. Rev. Lett.* **111**, 107006 (2013).
  - [11] R. M. Fernandes *et al.*, *Phys. Rev. Lett.* **105**, 157003 (2010).
  - [12] A. E. Böhrer *et al.*, *Phys. Rev. Lett.* **112**, 047001 (2014).
  - [13] Y. Gallais *et al.*, *Phys. Rev. Lett.* **111**, 267001 (2013).
  - [14] X. Xu *et al.*, *Phys. Rev. B* **81**, 224435 (2010).
  - [15] R. Okazaki *et al.*, *Science* **331**, 439 (2011).
  - [16] The torque has a zero value when fields point along high-symmetry directions (e.g., the  $c$ -axis) where the free energy has extreme value, recalling the torque is the first derivative of the free energy to angle.
  - [17] Z. Ren *et al.*, *Phys. Rev. Lett.* **102**, 137002 (2009).
  - [18] S. Jiang *et al.*, *New J. Phys.* **11**, 025007 (2009).
  - [19] H. S. Jeevan, D. Kasinathan, H. Rosner, and P. Gegenwart, *Phys. Rev. B* **83**, 054511 (2011).
  - [20] J. Maiwald, H. S. Jeevan, and P. Gegenwart, *Phys. Rev. B* **85**, 024511 (2012).
  - [21] S. Zapf *et al.*, *Phys. Rev. Lett.* **110**, 237002 (2013).
  - [22] S. Nandi *et al.*, *Phys. Rev. B* **89**, 014512 (2014).
  - [23] S. Jiang, H. S. Jeevan, J. Dong, and P. Gegenwart, *Phys. Rev. Lett.* **110**, 067001 (2013).
  - [24] C. Fang, H. Yao, W. F. Tsai, J. Hu, and S. A. Kivelson, *Phys. Rev. B* **77**, 224509 (2008).
  - [25] C. Xu, M. Müller, and S. Sachdev, *Phys. Rev. B* **78**, 020501(R) (2008).
  - [26] R. M. Fernandes, E. Abrahams, and J. Schmalian, *Phys. Rev. Lett.* **107**, 217002 (2011).
  - [27] R. M. Fernandes, A. V. Chubukov, J. Knolle, I. Eremin, and J. Schmalian, *Phys. Rev. B* **85**, 024534 (2012).
  - [28] R. M. Fernandes, A. V. Chubukov, J. Schmalian, *Nat. Phys.* **10**, 97 (2014).
  - [29] C. C. Lee, W. G. Yin, and W. Ku, *Phys. Rev. Lett.* **103**, 267001 (2009).
  - [30] W. Lv, J. Wu, and P. Phillips, *Phys. Rev. B* **80**, 224506 (2009).
  - [31] C. C. Chen *et al.*, *Phys. Rev. B* **82**, 100504 (2010).
  - [32] S. Thirupathaiah *et al.*, *Phys. Rev. B* **84**, 014531 (2011).
  - [33] R. M. Fernandes, S. Maiti, P. Wölfe and A. V. Chubukov, *Phys. Rev. Lett.* **111**, 057001 (2013).
  - [34] S. Jiang *et al.*, *J. Phys. Condens. Matter* **21**, 382203 (2009).

- [35] J. Dai *et al.*, Proc. Natl Acad. Sci. USA **106**, 4118 (2009).
- [36] K. Hashimoto *et al.*, Science **336**, 1554 (2012).
- [37] P. Walmsley *et al.*, Phys. Rev. Lett. **110**, 257002 (2013).
- [38] J. G. Analytis *et al.*, Nat. Phys. doi:10.1038/nphys2869.
- [39] R. M. Fernandes, and A. J. Millis, Phys. Rev. Lett. **111**, 127001 (2013).
- [40] R. M. Fernandes, and A. J. Millis, Phys. Rev. Lett. **110**, 117004 (2013).